

IMPROVING M_s ESTIMATES BY CALIBRATING VARIABLE-PERIOD MAGNITUDE SCALES AT REGIONAL DISTANCES

Jessie L. Bonner¹, Robert B. Herrmann², Michael E. Pasyanos³, Harley Benz⁴, and David G. Harkrider¹

Weston Geophysical Corporation¹, St. Louis University²,
Lawrence Livermore National Laboratory³, and the United States Geological Survey⁴

Sponsored by National Nuclear Security Administration

Contract Nos. DE-AC52-04NA25547^{1,2} and DE-FC52-06NA27320³
Proposal No. BAA04-63

ABSTRACT

During the final year of our project, we have calibrated the use of surface-wave magnitudes (M_s), measured at regional distances as a rapid and robust estimator of seismic moment. We have used the Russell (2006) variable-period surface-wave magnitude formula to convert M_s to seismic-moment magnitude, M_w , at local to regional distances using global datasets. In this pilot study, the Russell M_s technology was applied to 169 North American events with $3.2 < M_w < 6.5$ at distances ranging from 48 to 5,268 km. The technique uses a time-domain magnitude estimation procedure that employs zero-phase Butterworth filters to effectively measure Rayleigh-wave Airy phase amplitudes at local and near-regional distances (e.g., < 1000 km). This allows for surface wave magnitudes to be estimated within minutes of the initiation of a seismic event. Of the 7,370 event-station pairs, more than half (4,051) of the measurements were at distances < 1,000 km.

The M_s estimates were regressed against moment magnitudes (M_w) estimated from P -wave modeling and/or Rayleigh- and Love-wave spectral amplitudes (Herrmann et al., 2008). M_w can be estimated using the relationship: $M_w = 1.951 + 0.649 M_s$. The observed scatter in the estimated M_w was approximately ± 0.2 magnitude units. The residuals between true and M_s -predicted M_w have a definable faulting mechanism effect, especially when strike-slip events are compared to those with other mechanisms. Preliminary results suggest that our $M_s:M_w$ relationship for North America is also transportable to the Middle East and the Korean Peninsula.

We have also determined a methodology to estimate the M_s detection thresholds for the Russell formula. Broadband noise estimates for any seismic station, which are typically in units of acceleration m^2/s^3 and decibels, can be converted to nanometers (nm) and input into the Russell equation for variable-period surface waves. We propagate these noise estimates at periods (T) between 8 and 40 s to distances (Δ) between 1 and 40 degrees. The $M_s(T,\Delta)$ were estimated and contoured providing the optimal detection threshold for each station. We have estimated the $M_s(T,\Delta)$ for the stations of the Global Seismographic Network (GSN) using broadband noise estimates supplied by Berger et al. (2004).

OBJECTIVES

Developing a methodology for calculating surface wave magnitudes that is valid at both regional and teleseismic distances, applicable to events of variable sizes and signal-to-noise ratios, calibrated for variable structure and propagation, and easy to automate in an operational setting, is an important monitoring goal. Our objectives are to create such a methodology, and to use it to lower M_s estimation and detection thresholds. We hope that the method will provide a seamless tie between M_s estimation at regional and teleseismic distances.

To accomplish our objectives, we developed the Matlab program EVALSURF (Bonner et al., 2006), which estimates variable-period ($8 < T < 25$ s; recently updated to 40 s) Rayleigh-wave magnitudes using the Russell (2006) and M_s (VMAX) measurement technique (Bonner et al., 2006) for comparison to the historical formulas of Marshall and Basham (1972) and Rezapour and Pearce (1998). The program uses the updated Lawrence Livermore National Laboratory group velocity models for Eurasia (Pasyanos, 2005) to identify, phase match filter, and extract the fundamental-mode Rayleigh waves for analysis. During the past year, we calibrated the use of surface wave magnitudes (M_s), measured at regional distances as a rapid and robust estimator of seismic moment. We have also determined a methodology to estimate the M_s detection thresholds for European and Asian Global Seismographic Network (GSN) stations.

RESEARCH ACCOMPLISHED

Surface Wave Magnitudes

Many surface wave magnitude scales have been developed during the past century. They have either been based on empirical (Gutenberg, 1945; Vaněk et al., 1962; Marshall and Basham, 1972) or theoretical (Rezapour and Pearce, 1998; Stevens and McLaughlin, 2001) aspects of Rayleigh-wave propagation. Knowing how and when to apply these formulas has often been confusing, as some of these formulas were developed strictly for ~20-second surface waves at teleseismic distances. Others were developed for regional and teleseismic distances and variable periods (> 10 s). What was needed was a seamless relationship between estimating M_s at regional and teleseismic distances for events of a wider range of magnitudes.

Russell (2006) addressed this need by developing a time-domain method for measuring surface waves with minimal digital processing, using zero-phase Butterworth filters. The method can effectively measure surface-wave magnitudes at both regional and teleseismic distances, at variable periods between 8 and 25 s. The magnitude equation is

$$M_{s(b)} = \log(a_b) + \frac{1}{2} \log(\sin(\Delta)) + 0.003 \left[\left(\frac{20}{T} \right)^{1.8} \Delta - 0.66 \log \left(\frac{20}{T} \right) - \log(f_c) - 0.43 \right], \quad (1)$$

where a_b is the amplitude of the Butterworth-filtered surface waves (zero-to-peak in nanometers) and f_c is the filter frequency of a zero-phase Butterworth band-pass filter with corner frequencies $1/T-f_c$, $1/T+f_c$. At the reference period $T=20$ s, the equation is equivalent to Von Seggern's formula (1977) scaled to Vaněk et al. (1962) at 50 degrees. For periods $8 \leq T \leq 25$, the equation is corrected to $T=20$ sec, accounting for source effects, attenuation, and dispersion. This technique is often referred to as M_s (VMAX) for **V**ariable-period, **MAX**imum amplitude magnitude estimates (Bonner et al., 2006).

The advantages of the M_s (VMAX) technique include

- The technique allows for time-domain measurements of surface-wave amplitudes, giving an analyst the ability to easily and visually confirm that the pick is correct and is an actual Rayleigh wave.
- It allows for surface-wave magnitudes to be measured at local and regional distances where traditional 20-s magnitudes cannot be used. These magnitudes are not biased with respect to teleseismic estimates.
- The application of narrow-band Butterworth-filtering techniques appropriately handles the Airy phase.
- The method is variable period and not restricted to near 20-s period, and the analyst is allowed to measure the surface wave magnitude where the signal is largest.

M_s (VMAX) Methodology

To estimate M_s (VMAX), we apply a series of zero-phase 3rd-order Butterworth filters to the data with the corner frequencies $(1/T)-f_c, (1/T)+f_c$, where

$$f_c \leq \frac{G_{min}}{T\sqrt{\Delta}} \quad (2)$$

For continental paths between 8 and 25 s, G_{min} , which is based on dispersion effects, is set to 0.6. The center periods are placed at 1-second intervals between 8 and 25 s. We construct the envelope function of the filtered signal and measure the maximum zero-to-peak amplitude in a group velocity window between 2.0 and 4.0 km/s. An analyst then visually confirms that the correct waveform feature is being measured—a benefit of using a time-domain measurement. The procedure can be automated based on signal-to-noise requirements within the window. In Figure 1 we show examples of filter panels from an $M_w=4.83$ Montana earthquake recorded at station DUG at a near-regional distance of 509 km. Note the differences in the Rayleigh-wave amplitudes between 20-s periods, where traditional M_s is measured, and 8–14 s periods.

We record the maximum amplitude in each of the 18 filter bands and then use Equation 1 to calculate a variable-period surface-wave magnitude. As a result, 18 different magnitudes are estimated for each station recording the event (Figure 2). We then search the variable-period filtered data (Figure 1) to determine the period of the maximum Airy-corrected amplitude. We use the magnitude calculated at that period as the final estimate. As an example, the period of maximum amplitude for the DUG recording occurred at $T=10$ s. We note that for this Montana event, all of the M_s (VMAX) estimates were made at periods of less than 18 sec. We do the same processing for all stations that recorded the event and then estimate a network M_s (VMAX) (4.42), the interstation standard deviation (0.13), and surface-wave magnitude “noise” floors at each station (see Figure 2).

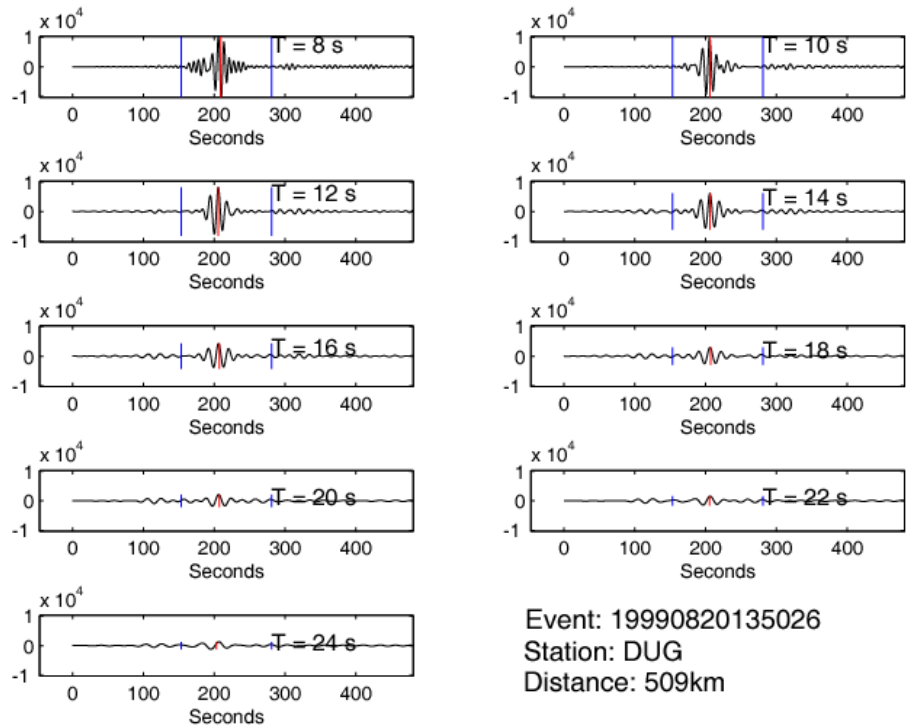


Figure 1. Filter combs of Rayleigh waves at periods of 8, 10, 12,...,24 seconds for a Montana earthquake recorded at DUG. The first blue line is 4.0 km/s, while the second is 2.0 km/s. The red line marks the largest amplitude. Amplitudes are in nm.

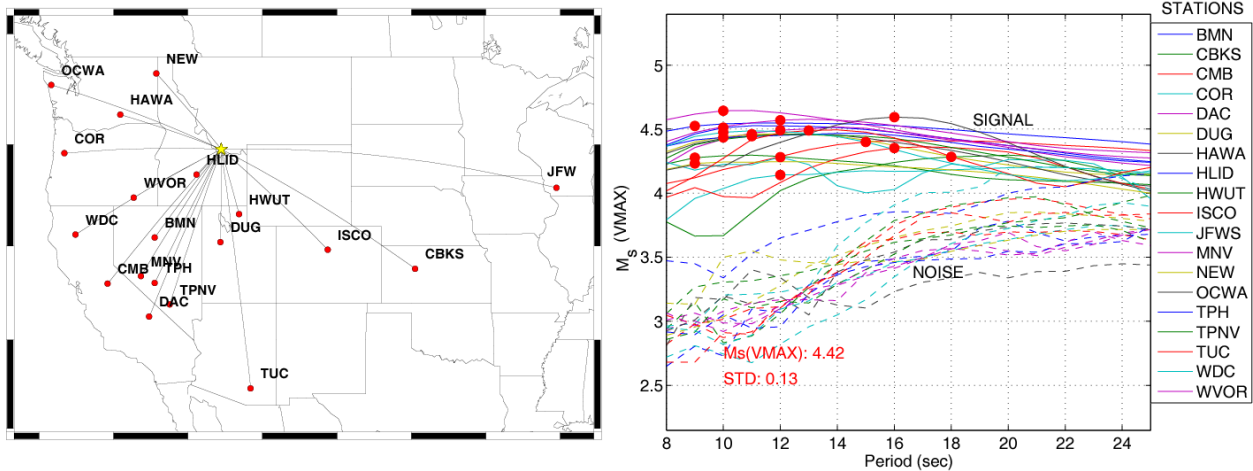


Figure 2. $M_s(\text{VMAX})$ results for the Rayleigh waves recorded from a Montana earthquake. The solid lines represent signals while the dashed lines are pre-surface-wave noise levels. The station magnitudes were averaged to form a network $M_s(\text{VMAX})$ of 4.42 for this $M_w=4.83$ event.

Application in North America

We have used the $M_s(\text{VMAX})$ method to estimate surface-wave magnitudes for 169 events in North America. The events were part of a database of North American events for which Herrmann et al. (2008) measured an M_w , using either broadband waveform modeling and/or Rayleigh- and Love-wave spectral amplitudes. The events include most types of faulting focal mechanisms (Zoback, 1992). Figure 3 shows the geographic distribution of these events, which were $3.2 < M_w < 6.5$, and stations. $M_s(\text{VMAX})$ was estimated for stations at distances ranging from 48 to 5,268 km. Of the 7,370 event-station pairs, 4,051 of the measurements were at distances $< 1,000$ km.

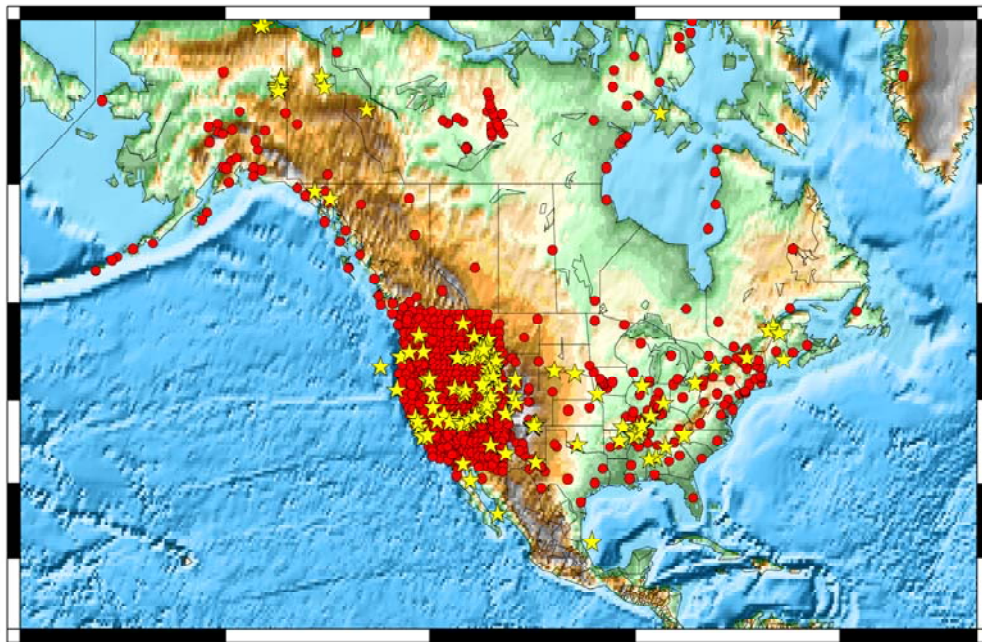


Figure 3. Earthquakes (yellow stars) and stations (red circles) used in a pilot study to examine the effectiveness of using regional surface-wave magnitudes to estimate M_w .

An example of the processing for the 21 February 2008 Wells, Nevada ($M_w=5.88$) event is shown in Figure 4. This event was located within the heart of Earthscope's Transportable Array, and thus was recorded on hundreds of stations within North America alone. Because the M_s (VMAX) technology can estimate unbiased surface wave magnitudes at epicentral distances as close as 50 km, we generated 506 surface-wave magnitude estimates for this event with only a very small azimuthal gap. Even though the focal mechanism for this normal fault event shows differences in the surface wave radiation patterns at 10, 15, 20, and 25 s (Herrmann et al., 2008), the radiation pattern of the M_s estimates shows no significant radiation patterns. This is due in part to the fact that the variable-period methodology picks the surface-wave estimate at the largest amplitude and often migrates away from periods with radiation pattern nulls. We determined an M_s (VMAX) of 5.99 for the event.

2008/02/21 14:16:05 41.076 -114.771 Nevada M_w : 5.88

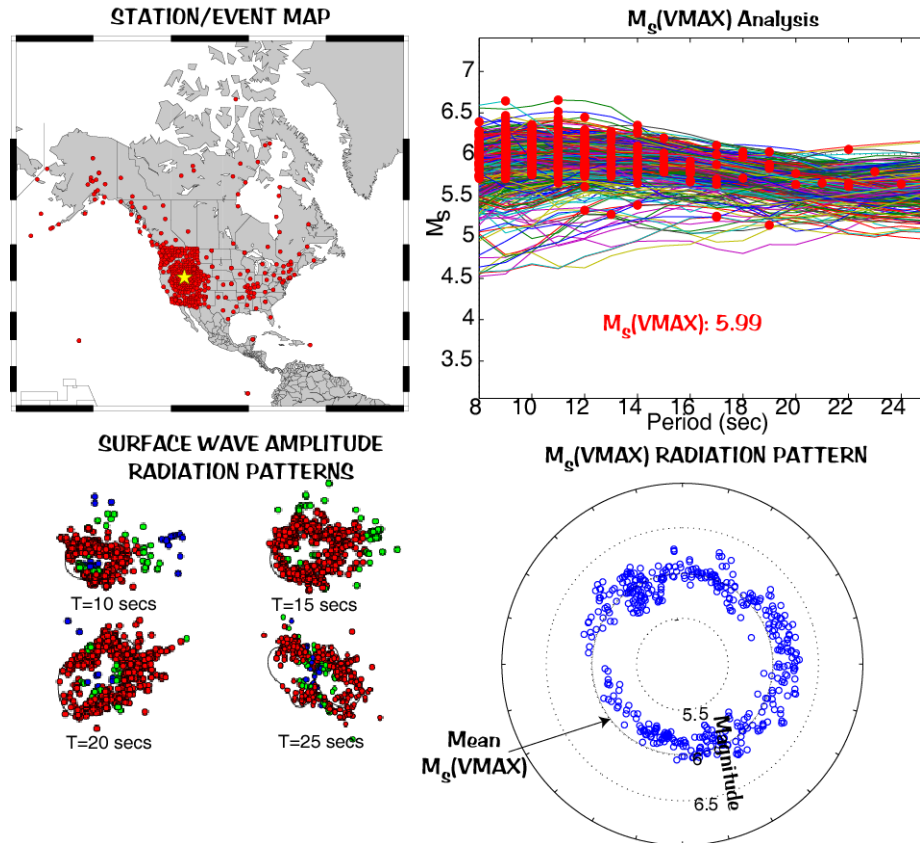


Figure 4. M_s (VMAX) estimation for the 21 February 2008 Wells, NV earthquake. Shown are the stations used to estimate the variable-period surface-wave magnitude, the magnitude analysis at periods between 8-25 seconds, surface wave radiation patterns from Herrmann et al. (2008), and the M_s estimates as a function of event-to-station azimuth.

Relationship Between M_w and M_s (VMAX)

We derived a relationship between M_w and M_s (VMAX) using the 169 North American earthquakes. The M_s estimates were regressed (Figure 5) against moment magnitudes (M_w) and $\log M_o$ estimated from P -wave modeling and/or Rayleigh- and Love-wave spectral amplitudes. M_w can be estimated using the relationship: $M_w = 1.951 + 0.649 M_s$. To demonstrate the observed scatter in the method, we show the residual M_s estimates as a function of period and distance in Figure 6. With the exception of $T=8$ sec, where highly variable crustal structure is problematic, the residual surface-wave magnitude estimates are almost always within ± 0.2 magnitude units of the mean value. And there are no significant distance trends observable in the data at periods greater than 10 sec.

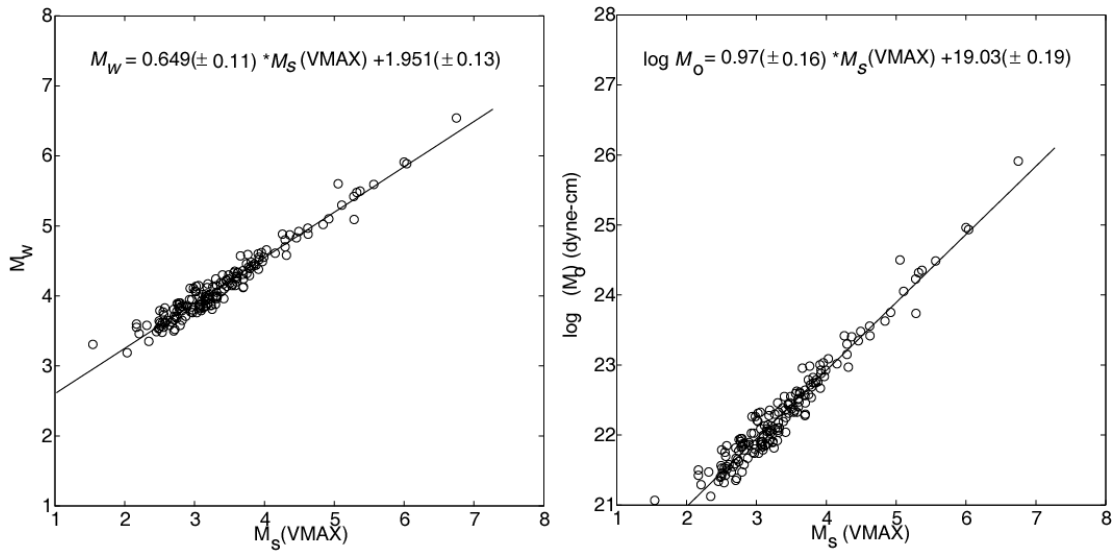


Figure 5. Linear regressions of M_w (left) and $\log M_o$ (right) versus $M_s(\text{VMAX})$. The moments were determined from body wave modeling and/or Love and Rayleigh-wave spectral amplitudes (Herrmann et al., 2008).

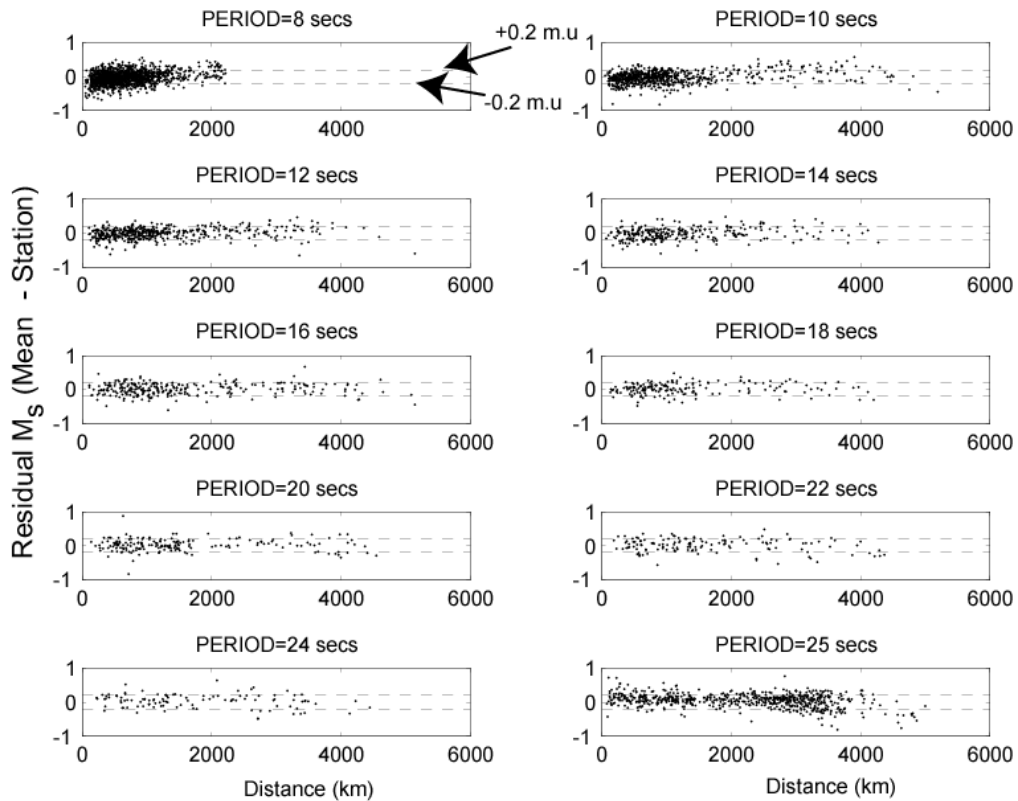


Figure 6. Scatter in the estimated $M_s(\text{VMAX})$ estimates as a function of the evaluation period and distance.

The scatter (Figure 7) between the observed and predicted M_w shows mechanism dependence for normal and strike-slip faulting sources. Each focal mechanism was classified as either normal (NF) strike-slip (SS), thrust (TF), or oblique-slip variations of normal and thrust faults using the Zoback (1992) classification scheme. For normal faults,

the predicted M_w is ~ 0.04 magnitude units larger than the observed M_w . A similar bias might be noted for thrust faulting as more estimates are obtained in the future. On the contrary, for strike-slip faults, the predicted estimate is ~ 0.07 magnitude units smaller than the observed M_w . The reason for these differences results from our M_s estimates only being based on the Rayleigh waves. Strike-slip events contain a significant amount of their moment from energy in the Love waves, which are not considered in our technique. The results show there is little, if any, depth dependence on the predicted M_w for events with crustal depths.

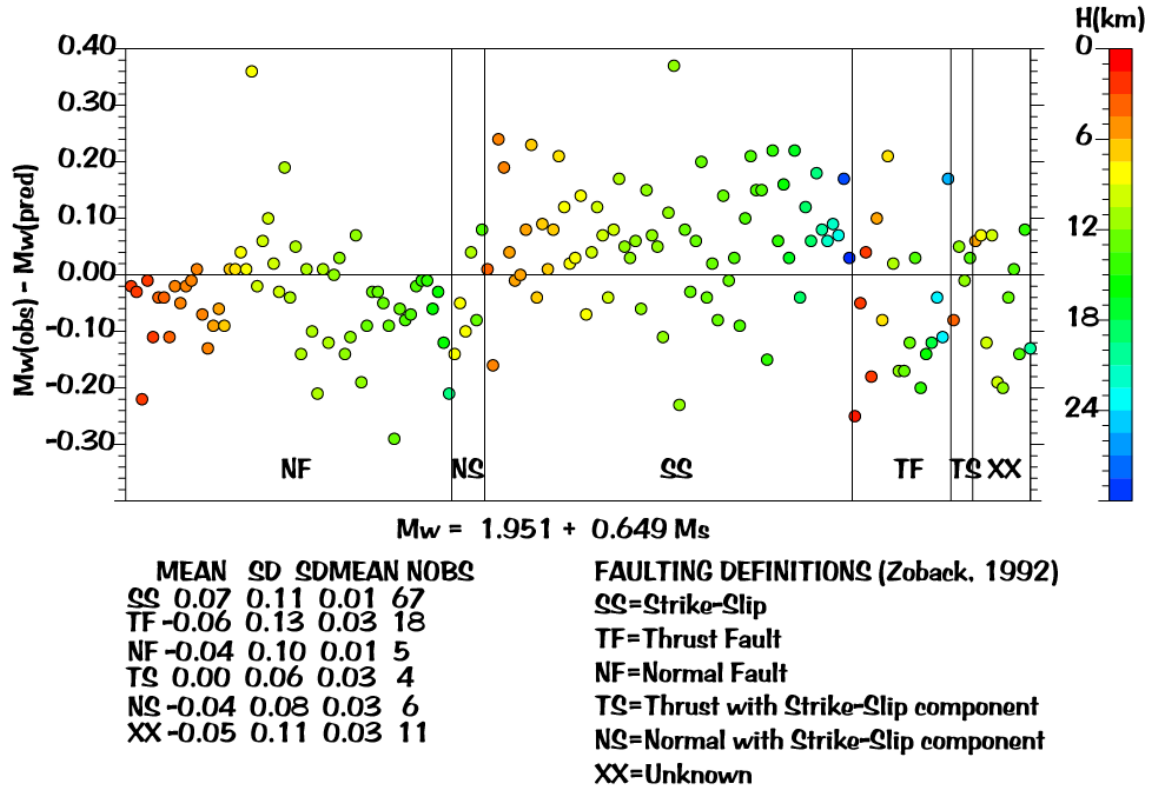


Figure 7. The dependence of the M_s -predicted M_w as a function of mechanism and depth. The mechanisms are based on the Zoback (1992) classification scheme. The residuals between the observed and M_s -predicted M_w have a definable faulting mechanism effect, especially when strike-slip events are compared to those with other mechanisms.

Predicting M_s (VMAX) Detection Thresholds

Broadband noise estimates can be used to estimate the M_s (VMAX) threshold floor for any seismic station. Berger et al. (2004) compiled broadband ambient noise estimates for the GSN. Peter Davis (Executive Director, Project IDA at the University of California, San Diego) provided us with the noise estimates for the GSN stations. As an example, the left subplot of Figure 8 shows the 25th percentile noise estimate for station AAK compared to the low noise model for the GSN.

We converted these noise estimates, which were in units of acceleration m^2/s^3 and decibels, to nanometers (nm) and input them into Equation 1 for variable-period surface waves. We propagated these noise estimates at periods (T) between 8 and 25 s to distances (Δ) between 1 and 60 degrees. The $M_s(T, \Delta)$ were estimated and contoured (right subplot of Figure 8). This colormap provides the optimal detection threshold for each station for a signal-to-noise ratio of 2. If the event has an M_s smaller than these values at a particular distance or period, we will probably discard it due to the inability to verify that it is a Rayleigh wave because of the "noise-based" M_s background level.

Using the GSN noise estimates (examples are shown in Figures 8 and 9), we determine the maximum distance in which we could record an $M_s=2.5$ and $M_s=3.0$. This distance is plotted as the radius of a circle centered on the station in Figures 10 and 11 for Europe and Asia. The blue circle shows the detection limits for the M_s (VMAX) technique, which considers periods between 8 and 25 s. The red circle shows detection distances if only periods between 17 and 23 s were considered, which is the traditional bandwidth for surface wave magnitude estimation. For $M_s=2.5$, the M_s (VMAX) technique has a mean detection distance of 9° compared with 7° for traditional 17–23-second measurements. For $M_s=3.0$, the mean detection distance is 26° for M_s (VMAX) and 22° for the traditional bandwidth.

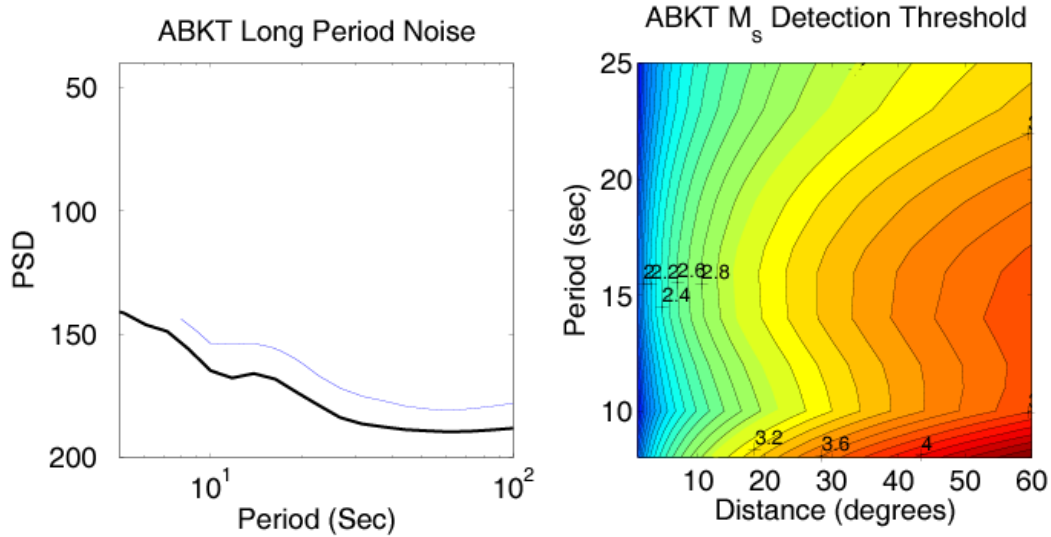


Figure 8. M_s (VMAX) detection threshold for station ABKT. Left: Long-period noise estimates (blue line) for the station compared to the GSN low noise model (solid black line). Right: Detection magnitude thresholds contoured as a function of distance and period.

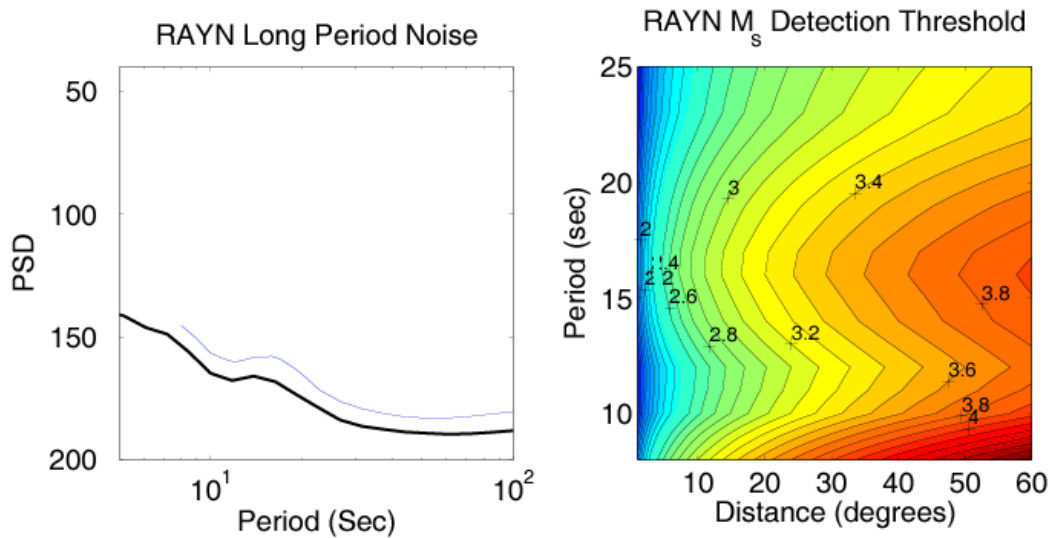


Figure 9. M_s (VMAX) detection threshold for station RAYN. Left: Long-period noise estimates (blue line) for the station compared to the GSN low-noise model (solid black line). Right: Detection magnitude thresholds contoured as a function of distance and period.

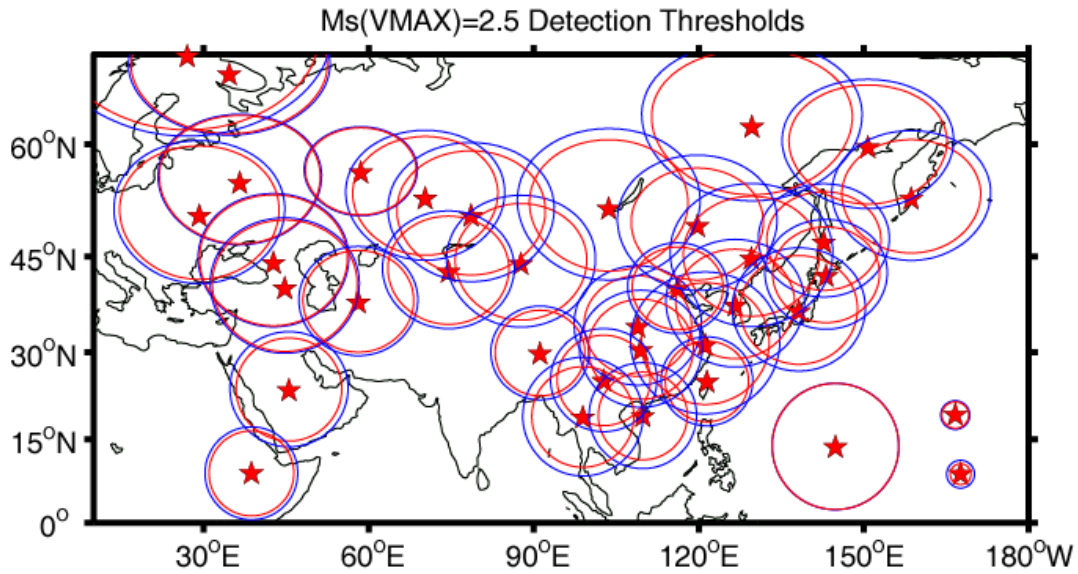


Figure 10. Detection thresholds for Europe and Asian GSN stations for an $M_s(\text{VMAX})=2.5$. The blue curve shows the detection threshold of $M_s(\text{VMAX})$ between 8- and 25-second periods. The red curve shows the detection thresholds only using 17–22-second surface waves, which is the traditional bandwidth for analysis.

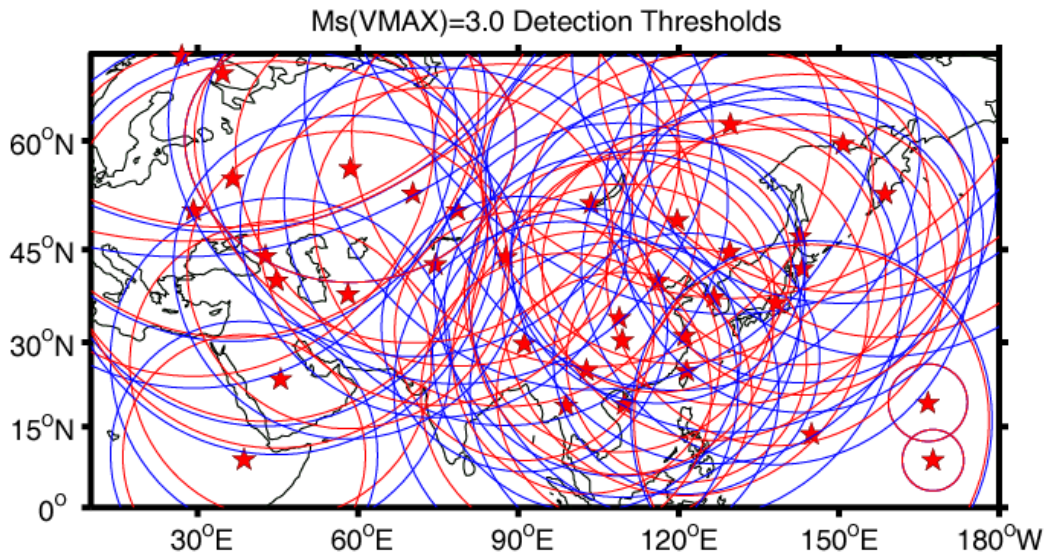


Figure 1

Figure 11. Detection thresholds for Europe and Asia for an $M_s(\text{VMAX})=3.0$.

CONCLUSIONS AND RECOMMENDATIONS

The variable-period surface wave magnitude $M_s(\text{VMAX})$ continues to provide a better and more consistent estimate of source size, particularly for smaller events and at shorter distances. During the past year, we applied $M_s(\text{VMAX})$ to 169 North American events with $3.2 < M_w < 6.5$ at distances ranging from 48 to 5,268 km. The M_s estimates were regressed against moment magnitudes (M_w) estimated from P -wave modeling and/or Rayleigh- and Love-wave spectral amplitudes. The resulting $M_s:M_w$ relationship has scatter on the order of ± 0.2 magnitude units in the estimated M_w . The residuals between true and M_s -predicted M_w have a definable faulting mechanism effect, especially when strike-slip events are compared to those with other mechanisms. This could have important

ramifications for the $M_s:m_b$ discriminant in regions where a particular mechanism dominates the seismicity. This exercise provides a tool for rapid M_w estimation of events with $M_w > 3.5$ for North America. Preliminary application of the same procedure to two other regions suggests that this $M_s:M_w$ relationship is also transportable to the Middle East and Korean Peninsula (Figure 12).

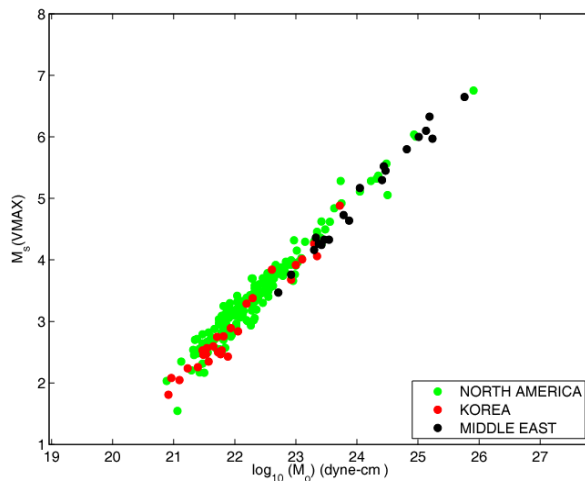


Figure 12. Comparison of $\log M_o$ versus $M_s(\text{VMAX})$ for earthquakes in North America (green), Korea (red) and the Middle East (black). Note that the Korean earthquakes are mostly strike-slip.

REFERENCES

- Berger, J., P. Davis, and G. Ekstrom (2004). Ambient earth noise: a survey of the Global Seismographic Network, *J. Geophys. Res.* 109: B11307.
- Bonner, J. L., D. Russell, D. Harkrider, D. Reiter, and R. Herrmann, (2006). Development of a Time-Domain, Variable-Period Surface Wave Magnitude Measurement Procedure for Application at Regional and Teleseismic Distances, Part II: Application and M_s-m_b Performance. *Bull. Seism. Soc. Am.* 96: 678 – 696
- Bonner, J., R. B. Herrmann, and H. Benz (2008). Rapid estimates of seismic moment using variable-period surface-wave magnitudes. *Seism. Res. Letts.* 79: 349.
- Gutenberg, B., (1945). Amplitudes of surface waves and the magnitudes of shallow earthquakes. *Bull. Seism. Soc. Am.* 35: 3.
- Herrmann, R. B., H. Benz, and C. Ammon (2008). Systematic moment tensor estimation for North America earthquakes. *Seism. Res. Letts.* 79: 349.
- Pasyanos, M. E. (2005). A variable-resolution surface wave dispersion study of Eurasia, North Africa, and surrounding regions, *J. Geophys. Res.* Vol. 110, No. B12, B12301 10.1029/2005JB003749.
- Rezapour, M., and R. G. Pearce, (1998). Bias in surface-wave magnitude M_s due to inadequate distance correction. *Bull. Seism. Soc. Am.* 88: 43–61.
- Russell, D. R., (2006). Development of a time-domain, variable-period surface wave magnitude measurement procedure for application at regional and teleseismic distances. Part I—Theory. *Bull. Seism. Soc. Am.* 96: 665–677.
- Marshall, P. D. and P. W. Basham, (1972). Discrimination between earthquakes and underground explosions employing an improved M_s scale. *Geophys. J. R. Astr. Soc.* 29: 431–458.
- von Seggern, D., (1977). Amplitude distance relation for 20-Second Rayleigh waves. *Bull. Seism. Soc. Am.* 67, 405–411.
- Stevens, J. L. and K.L. McLaughlin, (2001). Optimization of surface wave identification and measurement, in *Monitoring the Comprehensive Nuclear Test Ban Treaty: Surface Waves*, eds. Levshin, A. and M.H. Ritzwoller, *Pure Appl. Geophys.* 158: 1547–1582.
- Vaněk, J., A. Zatopek, V. Karnik, Y. V. Riznichenko, E. F. Saverensky, S.L. Solov'ev, and N.V. Shebalin, (1962). Standardization of magnitude scales. *Bull. (Izvest.) Acad. Sci. U.S.S.R., Geophys. Ser.* 2: 108.
- Zoback M. L.; 1992: First- and second-order patterns of stress in the lithosphere: the world stress map project, *J. Geophys. Res.* 97: 11703–11728.